

Association of Air Pollution with a Urinary Biomarker of Biological Aging and Effect Modification by Vitamin K in the FLEMENGHO Prospective Population Study

Dries S. Martens,¹ De-Wei An,^{2,3,4} Yu-Ling Yu,^{3,4} Babangida S. Chori,^{1,3} Congrong Wang,¹ Ana Inês Silva,¹ Fang-Fei Wei,⁵ Chen Liu,⁵ Katarzyna Stolarz-Skrzypek,⁶ Marek Rajzer,⁶ Agnieszka Latosinska,⁷ Harald Mischak,⁷ Jan A. Staessen,^{2,3,8*} and Tim S. Nawrot^{1,4*} (The FLEMENGHO Investigators)

¹Centre for Environmental Sciences, Hasselt University, Hasselt, Belgium

²Shanghai Institute of Hypertension, Ruijin Hospital, Shanghai Jiaotong University School of Medicine, Shanghai, China

³Non-Profit Research Association Alliance for the Promotion of Preventive Medicine, Mechelen, Belgium

⁴Research Unit Environment and Health, KU Leuven Department of Public Health and Primary Care, University of Leuven, Leuven, Belgium

⁵Department of Cardiology, The First Affiliated Hospital of Sun Yat-Sen University, Guangzhou, Guangdong, China

⁶First Department of Cardiology, Interventional Electrophysiology and Hypertension, Jagiellonian University, Kraków, Poland

⁷Mosaiques Diagnostics GmbH, Hannover, Germany

⁸Biomedical Sciences Group, Faculty of Medicine, University of Leuven, Leuven, Belgium

BACKGROUND: A recently developed urinary peptidomics biological aging clock can be used to study accelerated human aging. From 1990 to 2019, exposure to airborne particulate matter (PM) became the leading environmental risk factor worldwide.

OBJECTIVES: This study investigated whether air pollution exposure is associated with accelerated urinary peptidomics aging, independent of calendar age, and whether this association is modified by other risk factors.

METHODS: In a Flemish population, the urinary peptidomic profile (UPP) age (UPP-age) was derived from the urinary peptidomic profile measured by capillary electrophoresis coupled with mass spectrometry. UPP-age-R was calculated as the residual of the regression of UPP-age on chronological age, which reflects accelerated aging predicted by UPP-age, independent of chronological age. A high-resolution spatial-temporal interpolation method was used to assess each individual's exposure to PM₁₀, PM_{2.5}, black carbon (BC), and nitrogen dioxide (NO₂). Associations of UPP-age-R with these pollutants were investigated by mixed models, accounting for clustering by residential address and confounders. Effect modifiers of the associations between UPP-age-R and air pollutants that included 18 factors reflecting vascular function, renal function, insulin resistance, lipid metabolism, or inflammation were evaluated. Direct and indirect (via UPP-age-R) effects of air pollution on mortality were evaluated by multivariable-adjusted Cox models.

RESULTS: Among 660 participants (50.2% women; mean age: 50.7 y), higher exposure to PM₁₀, PM_{2.5}, BC, and NO₂ was associated with a higher UPP-age-R. Studying effect modifiers showed that higher plasma levels of desphospho-uncarboxylated matrix Gla protein (dpucMGP), signifying poorer vitamin K status, steepened the slopes of UPP-age-R on the air pollutants. In further analyses among participants with dpucMGP ≥ 4.26 $\mu\text{g/L}$ (median), an interquartile range (IQR) higher level in PM₁₀, PM_{2.5}, BC, and NO₂ was associated with a higher UPP-age-R of 2.03 [95% confidence interval (CI): 0.60, 3.46], 2.22 (95% CI: 0.71, 3.74), 2.00 (95% CI: 0.56, 3.43), and 2.09 (95% CI: 0.77, 3.41) y, respectively. UPP-age-R was an indirect mediator of the associations of mortality with the air pollutants [multivariable-adjusted hazard ratios from 1.094 (95% CI: 1.000, 1.196) to 1.110 (95% CI: 1.007, 1.224)] in participants with a high dpucMGP, whereas no direct associations were observed.

DISCUSSION: Ambient air pollution was associated with accelerated urinary peptidomics aging, and high vitamin K status showed a potential protective effect in this population. Current guidelines are insufficient to decrease the adverse health effects of airborne pollutants, including healthy aging trajectories. <https://doi.org/10.1289/EHP13414>

Introduction

Over the past 20 y, global life expectancy at birth increased from 67.2 to 73.5 y.¹ In line with this remarkable increase in longevity, global exposure to harmful environmental pollutants declined.² However, from 1990 to 2019, particulate matter (PM) shifted from the fifth rank to the most perilous environmental risk factor and

is associated with a 67.7% increase in the number of disability-adjusted life-years (DALYs).

PM with an aerodynamic diameter ≤ 10 μm (PM₁₀) is fractionated into PM with an aerodynamic diameter ≤ 2.5 μm (PM_{2.5}), referred to as fine particulate; within this fraction, ultrafine particles (<0.1 μm) reach the smallest airways and alveoli and have been shown to cross the blood–air barrier.³ Black carbon (BC), a constituent of PM, is generated through the incomplete combustion of fossil fuels and biomass, resulting in a sooty residue which, after inhalation, has been detected in urine, reproductive organs,⁴ placenta, and fetal organs.⁵ In addition to particulates, the air pollution mixture contains gaseous pollutants such as nitrogen dioxide (NO₂).

Aging is a heterogenic phenotype with varying inputs from genetic, cellular, and biochemical processes.⁶ Hallmarks of the insults caused by environmental pollutants greatly overlap with the molecular features of aging, indicating a tight connection between exposure, aging, and disease outcomes.⁷ Air pollutants have been associated with chronic inflammation and increased oxidative stress, and these are key mechanisms shared by accelerated aging.⁸ The latter is evidenced by associations observed between air pollution exposure and markers of accelerated biological aging, including shorter telomere lengths,⁹ mitochondrial dysfunction,¹⁰ higher epigenetic age.¹¹

*Joint senior authors who contributed equally.

Address correspondence to Jan A. Staessen, Alliance for the Promotion of Preventive Medicine, Leopoldstraat 59, BE 2800 Mechelen, Belgium. Telephone: +32-15-41-1747, +32-47-632-4928 (cell). Facsimile: +32-15-41-4542. Twitter: [jasta49](https://twitter.com/jasta49). Email: jan.staessen@appremed.org

Supplemental Material is available online (<https://doi.org/10.1289/EHP13414>).

H.M. is the cofounder and co-owner of Mosaiques Diagnostics (Hannover, Germany). A.L. is an employee of Mosaiques-Diagnostics. All other authors declare no competing interests.

Received 31 May 2023; Revised 28 September 2023; Accepted 15 November 2023; Published 11 December 2023.

Note to readers with disabilities: *EHP* strives to ensure that all journal content is accessible to all readers. However, some figures and Supplemental Material published in *EHP* articles may not conform to 508 standards due to the complexity of the information being presented. If you need assistance accessing journal content, please contact ehpsubmissions@niehs.nih.gov. Our staff will work with you to assess and meet your accessibility needs within 3 working days.

Urine contains more than 20,000 endogenous peptides, which are partly generated along the nephron or which pass into the tubular fluid through the glomerular barrier.¹² Sequencing these urinary peptides identifies the parental proteins. Thus, the urinary peptidomic profile (UPP) provides a body-wide molecular signature of ongoing pathophysiological processes.¹² Recently, a UPP aging clock (UPP-age) that includes 54 age-related urinary peptides was developed.¹³ Accelerated urinary peptidomic aging (reflected by a higher UPP-age-R, which is the UPP-age residualized on chronological age) was observed in patients with diabetes, COVID-19, or chronic kidney disease and predicted all-cause and cardiovascular mortality in the general population.¹³ To our knowledge no previous study has addressed how environmental insults, and ambient air pollution in particular, affect the UPP landscape and, therefore, how UPP might be applied in monitoring the health effects of environmental contaminants. To address this knowledge gap, data from a population cohort with long-term follow-up were analyzed.¹³ The research focused on the relation of the multidimensional UPP biomarker of accelerated aging (UPP-age-R)¹³ with long-term exposure to PM₁₀, PM_{2.5}, BC, and NO₂. Risk factors may enhance susceptibility to air pollution-induced molecular effects, and therefore potential effect modifiers (including risk biomarkers for vascular function, renal function, insulin resistance, lipid metabolism and inflammation) of the association between accelerated UPP aging and air pollution were tested. Finally, the mediating role of accelerated UPP aging in the link between air pollution exposure and mortality in vulnerable subgroups of the population was evaluated.

Methods

Study Design and Population

This study used data from the prospective population Flemish Study on Environment, Genes, and Health Outcomes (FLEMENGHO), which complies with the Helsinki declaration and is registered at the Belgian Data Protection Authority (III 11/1234/13; 22 August 2013). General study procedures have been outlined in detail previously.^{13,14} The ethics committee of the University Hospitals Leuven, Belgium, approved the secondary use of FLEMENGHO data (B32220083510).¹³ From 20 August 1985, to 14 December 1990 (Figure S1), a random sample of the households living in a geographically defined area of northern Belgium (Figure S2) was investigated with the goal to recruit an equal number of participants in each of six subgroups stratified by sex and age (20–39 y, 40–59 y, and ≥60 y of age). All household members 20 y of age or older were invited to take part, provided that the quota of their sex-age group had not yet been satisfied. From 3 April 1996 to 12 May 2004, recruitment of families continued, including young people 10–19 y of age. Participants younger than 18 y provided informed assent, and their parents or custodians gave informed consent (Figure S1). Of 4,286 people invited to participate in FLEMENGHO, 3,343 consented (participation rate: 78.0%). From 30 May 2005 until 31 May 2010, participants were invited to a follow-up examination, if their last known address was within 15 km of the local examination center (Eksel, Belgium) and if they had not withdrawn consent in any of the previous examination cycles (1985–2004).

The current study includes 828 FLEMENGHO participants who renewed consent for the 2005–2010 reexamination. Of these, 168 were excluded from analysis, because UPP had not been performed ($n = 24$), because they had outlying [three standard deviations (SDs) greater than the mean of all consenting participants] values of body mass index (BMI), plasma glucose, or serum creatinine ($n = 17$), or because modeled air pollution data were unavailable ($n = 127$). Thus, the study sample statistically analyzed 660 participants (Figure S3).

Clinical and Biochemical Measurements

All clinical, biochemical measurements and urine sample collections were performed once during the 2005–2010 follow-up visit (Figure S1). The date of urine collection during this study phase served as the baseline for mortality follow-up. Blood pressure was the average of five consecutive auscultatory readings obtained after participants had rested for 5 min in a seated position. Study nurses administered a standardized questionnaire about each participant's medical history, smoking (yes/no), and intake of antihypertensive drugs (yes/no). Antihypertensive drugs included diuretics (thiazides, loop diuretics, and aldosterone antagonists), beta-blockers, inhibitors of the renin-angiotensin system (angiotensin converting enzyme inhibitors and angiotensin receptor blockers), vasodilators (calcium-channel blockers and alpha-blockers), and other blood pressure-lowering agents. Waist circumference was measured to the nearest centimeter. Body fat percentage was measured using bioelectrical impedance (Bodystat QuadScan 4000, Bodystat).

Venous blood samples were obtained during the 2005–2010 clinical examination, after 8 h of fasting. After centrifugation and aliquoting, blood-derived specimens were stored at -80°C . On average, 1 wk after visiting the local examination center, participants collected at home an exactly timed 24-h urine sample in a 2,500-mL wide-neck plastic container (Sarstedt article number 77.576). Sodium azide (3 g) was added as preservative. Participants were asked to store bottles in a cool place (i.e., in a cellar, outside). After sample collection, the urine was mixed and divided in $5 \times 10\text{-mL}$ aliquots. Aliquots were stored at -40°C upon analysis. A single certified laboratory assessed the routine biochemistry, using quality-controlled automated methods. The estimated glomerular filtration rate (eGFR) was computed from serum creatinine, measured by a modification of Jaffe's methods with isotope-dilution calibration.¹⁵ According to the Chronic Kidney Disease Epidemiology Collaboration equation,¹⁶ $\text{eGFR} = 141 \times \text{minimum} (\text{S crt}/\kappa, 1) \alpha \times \text{maximum} (\text{S crt}/\kappa, 1)^{-1.209} \times 0.993 \text{ age} \times 1.018$ (if female), where S crt is the serum creatinine concentration in $\mu\text{mol/L}$, κ is 61.9 for women and 79.6 for men, and α is -0.329 for women and -0.411 for men; minimum indicates the minimum of S crt/ κ or 1 and maximum indicates the maximum of S crt/ κ or 1. Homeostatic Model Assessment for Insulin Resistance (HOMA-IR)¹⁷ was calculated from fasting glucose and insulin. Circulating biomarkers reflecting vascular function [vascular endothelial growth factor (VEGF) and Plasminogen activator inhibitor-1 (PAI1)], lipid metabolism (leptin and resistin), inflammation [C-reactive protein, tumor necrosis factor- α (TNF α), and tumor necrosis factor receptor 1 (TNFR1)], and renal injury [neutrophil gelatinase-associated lipocalin (NGAL)] were measured within 1 h of defrosting on a single serum aliquot, using Bio-Chip Array Technology by Randox Laboratories Ltd. Desphospho-uncarboxylated matrix Gla protein (dpucMGP), a biomarker reflecting vitamin K status, was measured on citrated plasma by enzyme-linked immunosorbent assay (ELISA).¹⁸ Higher dpucMGP values indicate poor vitamin K status.¹⁸

Demographic Measurements

Socioeconomic status was coded according to the comprehensive scale published by the UK Office of Population Censuses and Surveys.¹⁹ The 20 categories of the UK scale¹⁹ were inverted and recoded to grades ranging from 1 to 3, which reflected the hierarchy from the least to the most affluent layers of the population.²⁰ Based on the home address, the study participants were assigned to 148 statistical sectors with an average surface of 1.55 km^2 ; these sectors are the smallest units for which the National Institute of Statistics (www.statbel.fgov.be/en) compiles information on average on 643 items. The data resource was interrogated to obtain the median annual household income data by sector (2012).

Incidence of Mortality

At annual intervals, the vital status of FLEMENGHO participants was ascertained by record linkage with the National Population Registry in Brussels, Belgium. The *International Classification of Diseases, 10th edition* (ICD-10) codes for cause of death were obtained from the Flemish Registry of Death Certificates. All-cause (ICD-10: A00–Y89) and cardiovascular mortality (ICD-10: I00–I99) were the co-primary end points. The cause of death was validated against the records held by general practitioners, or the digital records maintained by four regional hospitals and the University Hospitals Leuven, all serving the catchment area. The date of urine collection in 2005–2010 served as the baseline, and surviving participants were censored on 30 June 2019.

Urinary Peptidomics Profiling and Definition of UPP-age-R

Sample preparation and CE-MS analysis. Sample preparation and capillary electrophoresis–mass spectrometry (CE-MS) analysis were performed essentially as described.²¹ Stored 10-mL urine aliquots were thawed and 700 μ L urine was mixed with 700 μ L of 2 M urea and 10 mM NH_4OH containing 0.02% sodium dodecyl sulfate (SDS). Subsequently, samples were ultrafiltered using a Centrstat 20 kDa cutoff centrifugal filter device (Satorius) to eliminate high molecular weight proteins. The obtained filtrate was desalted against 2 mM NH_4OH using a PD 10 gel filtration column (GE Healthcare Bio-Sciences Corp.) to remove urea, electrolytes and salts as well as to enrich polypeptides. The samples were lyophilized and stored at 4°C before usage. Shortly before CE-MS analysis, the samples were resuspended in 10 μ L high-performance liquid chromatography (HPLC)-grade H_2O .

A P/ACE MDQ capillary electrophoresis system (Beckman Coulter) was coupled with a MicrOTOF compact MS (Bruker Daltonics, Inc.) using an Agilent Technologies ESI Sprayer. A solution of 20% acetonitrile (Sigma-Aldrich) in HPLC-grade water (Roth) supplemented with 0.94% formic acid (Sigma-Aldrich) was used as running buffer. Capillaries (Polymicro) were uncoated fused silica, 50 μ m inner diameter (360 μ m outer diameter), with 90-cm length, and rinsed with running buffer (20% methanol, 0.94% formic acid) for 3 min prior to sample injection. Samples were injected into CE-MS with 2 psi for 99 s, resulting in injection volumes of \sim 280 nL. Separation was performed by applying 25 kV on the injection side (resulting in a current of \sim 13 μ A), and the capillary temperature was set to 35°C for the entire length of the capillary up to the ESI interface. After each analysis, the CE capillary was rinsed for 5 min with 0.1 M NaOH, followed by a 5-min wash with water and subsequently with running buffer. For CE-MS analysis, the electrospray ionization voltage was between 4.0 to 4.5 kV. Spectra were recorded over an m/z range of 350–3,000 and accumulated every 3 s.

CE-MS data processing. After the CE-MS analysis, mass spectral ion peaks representing identical molecules at different charge states were deconvoluted into single masses using MosaFinder software.²² Only signals with $z > 1$ observed in a minimum of three consecutive spectra with a signal-to-noise ratio of at least 4 were considered. The resulting peak list characterizes each polypeptide by its mass and migration time. Data were calibrated using 3,151 internal standards as reference data points for mass and migration time by applying global and local linear regression, respectively. Reference signals of 29 abundant peptides were used as internal standards for calibration of signal intensity using local linear regression.²³ These 29 endogenous “house-keeping” peptides were selected based on their high abundance and lack of association with disease. This procedure is highly

reproducible and addresses both analytical and dilution variances in a single calibration step. The latter approach outperforms standardization based on the urinary creatinine concentration, which only accounts for sample dilution as previously described in detail.²³ To ensure comparable performance, a standard urine sample is analyzed every second day as quality control. The performance of the analytical platform was assessed and described in detail previously.²¹ In short, among 60 independent analytic runs of a single urine sample, the coefficient of variation was 1%.²⁴ The obtained peak list characterizes each polypeptide by its calibrated molecular mass (Da), calibrated CE migration time (min), and normalized signal intensity. All detected peptides were deposited, matched, and annotated in a Microsoft SQL database, allowing further statistical analysis.

Sequencing of peptides. Peptides were sequenced using CE-MS/MS or liquid chromatography–tandem mass spectrometry (LC-MS/MS) analysis, as described in detail.¹² MS/MS experiments used an Ultimate 3000 nano-flow system (Dionex/LC Packings) or a P/ACE MDQ capillary electrophoresis system (Beckman Coulter), both connected to a Q Exactive Plus Hybrid Quadrupole-Orbitrap Mass Spectrometer (ThermoFisher Scientific). The mass spectrometer is operated in data-dependent mode to automatically switch between MS and MS/MS acquisition. Survey full-scan MS spectra (from m/z 300–2000) were acquired in the Orbitrap. Ions were sequentially isolated for fragmentation. Data files were searched against the UniProt human nonredundant database using Proteome Discoverer 2.4 and the SEQUEST search engine. Relevant settings were no fixed modifications, and oxidation of methionine and proline as variable modifications. The minimum precursor mass was set to 790 Da and the maximum precursor mass set to 6,000 Da with a minimum peak count of 10. The high-confidence peptides were defined by cross-correlation ($X_{\text{corr}} > 1.9$ and rank = 1. The false discovery rate (FDR) was set to 1%, and the precursor mass tolerance and fragment mass tolerance were 5 ppm and 0.05 Da, respectively. For further validation of obtained peptide sequences, the correlation between peptide charge at the working pH of 2 and CE-migration time was used to minimize false-positive derivation rates.²⁵ Calculated CE-migration time of the sequence candidate based on its peptide sequence (number of basic amino acids) was compared to the experimental migration time.

Calculation of UPP-age-R. Urinary peptidomics profiling as described above was used to develop a urinary peptidomics clock of aging as described in detail previously.¹³ In brief, in a first step, UPP-age was calculated as the linear combination of 54 age-associated urinary peptides derived from 17 proteins, using elastic net regression coefficients and intercept of the trained model relating UPP-age with chronological age as defined previously (details of the used coefficients for calculating UPP-age are provided in Table S1).¹³ As an index of accelerated aging independent of chronological age, UPP-age-R was calculated as the residual of the regression of UPP-age on chronological age (Figure S4).

Residential Ambient Air Pollution

The exposure of individual FLEMENGHO participants to PM_{10} , $\text{PM}_{2.5}$, BC, and NO_2 (in $\mu\text{g}/\text{m}^3$) was modeled from each participant’s residential address at the time of the air quality measurements (2010–2014). Air pollution levels were estimated using a high-resolution spatial-temporal interpolation method (kriging)²⁶ that takes into account land-cover data obtained from satellite images [CORINE database (<https://www.eea.europa.eu/publications/CORINELandcover>)] and pollution data of fixed monitoring stations in combination with a dispersion model.^{27,28} This approach provides daily exposure values calculated on a dense irregular receptor grid and interpolated to a 10-m \times 10-m raster, using input from the Belgian

telemetric air quality networks and emissions from point- (e.g., industries) and line sources (e.g., highways). The air quality network includes 65 monitoring stations for PM₁₀, 34 for PM_{2.5}, 14 for BC, and 44 for NO₂. Models covered daily estimated air pollution data averaged over a 5-y period (2010–2014), which reflects the long-term spatial air pollution and is representative of earlier periods.^{29–33} Model performance was evaluated by leave-one-out cross-validation across monitoring stations. The spatiotemporal explained variance was 70% for PM₁₀, 80% for PM_{2.5}, 74% for BC, and 78% for NO₂.

Statistical Analyses

Database management and statistical analysis were done using SAS (version 9.4; SAS Institute Inc.; maintenance level 5). The Kolmogorov-Smirnov test was applied to test deviation from the normal distribution. The distributions of biomarkers were rank normalized by sorting measurements from the smallest to the highest value and then applying the inverse cumulative normal function.³⁴ However, to keep consistency with previous FLEMENGHO publications, the distribution of γ -glutamyltransferase was logarithmically transformed. The central tendency and spread of continuously distributed variables were presented as mean \pm SD, geometric mean [interquartile range (IQR)] for γ -glutamyltransferase, or median (IQR), as appropriate. *p*-Values for the trends across thirds of PM₁₀ distribution were evaluated by linear regression or Cochran-Armitage trend test where appropriate. Pearson correlation coefficients or Spearman rank correlations were applied to express associations between variables. Statistical significance was a two-sided *p*-value of 0.05 or less.

The association of UPP-age-R with air pollutants was assessed using a generalized linear mixed model, accounting for the clustering between individuals sharing the same residential address as a random effect. In addition, the model accounted for sex, age, BMI, mean arterial pressure, plasma glucose, γ -glutamyltransferase (marker of excessive alcohol intake³⁵) current smoking, the total-to-high-density lipoprotein serum cholesterol ratio, eGFR, and socioeconomic status as fixed effects. For reasons of consistency with previous analyses in the FLEMENGHO population,^{13,36} covariables were selected *a priori* showing a potential link with air pollution exposure and UPP-age-R. The multivariable-adjusted associations between UPP-age-R and air pollutants were expressed as a difference in UPP-age-R (in years) for an IQR higher level in the air pollutant. Q-Q plots of the residuals were used to evaluate the assumptions of linear models.

Effect modification of how risk markers might affect the multivariable-adjusted relation of UPP-age-R with air pollutants was formally tested by introducing a statistical interaction term, UPP-age-R \times risk marker in the mixed models. A two-pronged approach was followed. The interaction was first tested for each individual risk marker. Next, principal component analysis was applied to generate summary variables that grouped risk markers for vascular function [systolic and diastolic blood pressure, VEGF, PAI1, and vitamin K status (dpucMGP)], renal function (eGFR and NGAL), insulin resistance (plasma glucose, serum insulin, and HOMA-IR), lipid metabolism (BMI, waist circumference, percentage body fat, leptin and resistin), and inflammation (high-sensitive C-reactive protein, TNF α , and TNFR1). Because dpucMGP showed a strong interaction with air pollution exposure, the UPP-age-R, air pollution association was further evaluated in analyses stratified by the median of dpucMGP. Sensitivity analyses addressed the consistency of the associations between UPP-age-R and air pollution by dpucMGP stratification. First, sex stratification was performed, because biological aging differs between men and women, as evidenced by biological changes women experience when they transition to postmenopausal status and by the longer life expectancy of women in comparison with men. Second, we

evaluated whether intake of vitamin K antagonists influenced our results by excluding participants who used vitamin K antagonists (coumarins). Third, we evaluated whether effect modification was not driven by diabetic patients, who are more vulnerable to air pollution, or by smoking status. Smokers inhale additional toxic particles. Finally, because vitamin K levels and air pollution may have a large socioeconomic related component, we adjusted for the median annual income per cluster as an additional socioeconomic variable. Because air pollution exposure is related to a higher UPP-age-R and we previously showed that a higher UPP-age-R is a predictor of total and cardiovascular mortality independent of chronological age,¹³ we therefore explored whether UPP-age-R is a potential mediator linking air pollution to mortality. For mediation analysis we used a published SAS macro for survival data as described by Valeri and VanderWeele.³⁷ This procedure was accomplished by decomposing the total effect into a direct effect (i.e., air pollution effect on mortality at a fixed level of the mediator, UPP-age-R) and an indirect effect (i.e., air pollution effect on mortality that operates through the mediator, UPP-age-R). These direct and indirect effects were estimated from multivariable-adjusted proportional hazards regression models for an IQR increment in air pollution exposure.

Results

Study Population Characteristics

All FLEMENGHO participants were White Europeans and at baseline (2005–2010) had a mean age of 50.7 y (SD: 15.4; range: 16.2–85.1 y). The cohort included 331 women (50.2%), 272 patients with hypertension (41.2%), of whom 167 (61.4%) were on antihypertensive drug treatment, and 23 patients with diabetes (3.5%). The annual mean air pollution levels were 18.0 $\mu\text{g}/\text{m}^3$ (IQR: 16.2–20.0 $\mu\text{g}/\text{m}^3$) for PM₁₀, 13.0 $\mu\text{g}/\text{m}^3$ (12.3–13.9 $\mu\text{g}/\text{m}^3$) for PM_{2.5}, 0.74 $\mu\text{g}/\text{m}^3$ (0.59–0.90 $\mu\text{g}/\text{m}^3$) for BC, and 17.2 $\mu\text{g}/\text{m}^3$ (14.5–19.8 $\mu\text{g}/\text{m}^3$) for NO₂. The Pearson correlation coefficients between the levels of the air pollutants ranged from 0.88 to 0.97 (Table S2). UPP-age was strongly correlated with chronological age (Pearson $r = 0.86$; $p < 0.0001$; Figure S4). Evaluation of the characteristics of participants across thirds of the distribution of the annual mean air pollution levels, using PM₁₀ as marker, revealed significant trends ($p \leq 0.015$) in means of age and various age-related variables (Table 1). Chronological age (46.5 y vs. 53.4 y), UPP-age (47.6 y vs. 52.6 y), systolic blood pressure (125.9 vs. 128.7 mm Hg), mean arterial pressure (94.8 vs. 95.6 mm Hg), plasma glucose (4.78 vs. 4.98 mmol/L), and total serum cholesterol (5.11 vs. 5.24 mmol/L) were lower in the highest air pollution level in comparison with the lowest. Conversely eGFR was higher (89.1 vs. 81.6 mL/min/1.73 m²) at higher air pollution levels. UPP-age-R was not associated with the air pollution categories ($p = 0.50$). The median annual income averaged per statistical sector (24.4 vs. 24.9 k€) was lower for participants in the higher air pollution category (Table 1). Similar trends were observed when using thirds of the PM_{2.5}, BC, or NO₂ distribution (Tables S3–S5).

Accelerated Urinary Peptidomics Aging in Association with Air Pollution

In both unadjusted and fully adjusted analyses, accelerated aging as captured by UPP-age-R was positively associated with PM₁₀, PM_{2.5}, BC, and NO₂ (Table 2). In fully adjusted models, a higher UPP-age-R was observed for an IQR higher level in the air pollutant, which amounted to 1.04 y (95% CI: 0.11 to 1.98 y; $p = 0.029$) for PM₁₀, 1.17 y (95% CI: 0.16 to 2.18 y; $p = 0.023$) for PM_{2.5}, 1.02 y (95% CI: 0.08 to 1.97 y; $p = 0.034$) for BC, and 0.87 y (95% CI: –0.01 to 1.74 y; $p = 0.051$) for NO₂ (Table 2).

Table 1. Characteristics of 660 FLEMENGHO participants by thirds of the distribution of averaged annual (2010–2014) PM₁₀ levels.

Characteristic	Low	Medium	High	<i>p</i> -Value
PM ₁₀ limits, µg/m ³	13.3 to <16.4	16.4 to <19.0	19.0–22.9	NA
Number in category	219	220	221	NA
Number of participants (%)				
Sex				0.72
Women	113 (51.6%)	112 (50.9%)	106 (48.0%)	
Men	106 (48.4%)	108 (49.1%)	115 (52.0%)	
Smoking				0.83
Yes	40 (18.3%)	45 (20.5%)	44 (19.9%)	
No	179 (81.7%)	175 (79.5%)	177 (80.1%)	
Hypertension				0.0053
Yes	91 (41.6%)	107 (48.6%)	74 (33.5%)	
No	128 (58.4%)	113 (51.4%)	147 (66.5%)	
Antihypertensive drug intake	59 (26.9%)	61 (27.7%)	47 (21.3%)	0.23
Diabetes mellitus				0.11
Yes	12 (5.5%)	7 (3.2%)	4 (1.8%)	
No	207 (94.5%)	213 (96.8%)	217 (98.2%)	
Mean ± SD of characteristic				
Age, years	53.4 (14.6)	52.6 (14.6)	46.5 (15.9)	<0.0001
UPP-age, years	52.6 (13.4)	52.2 (14.2)	47.6 (13.8)	0.00015
UPP-age-R, years	−0.40 (6.4)	−0.11 (8.1)	0.37 (6.4)	0.50
Body mass index, kg/m ²	26.3 (4.0)	26.4 (3.8)	26.4 (4.4)	0.96
Waist circumference, cm	89.9 (12.4)	90.3 (11.4)	90.0 (13.2)	0.95
Systolic pressure, mm Hg	128.7 (17.5)	132.2 (17.6)	125.9 (16.1)	0.00063
Diastolic pressure, mm Hg	79.1 (10.0)	80.4 (9.5)	79.3 (9.5)	0.29
Mean arterial pressure, mm Hg	95.6 (11.1)	97.7 (10.4)	94.8 (10.3)	0.015
Demographic variables				
Socioeconomic status, grade	1.21 (0.62)	1.25 (0.62)	1.30 (0.67)	0.34
Median annual income, k€	24.9 (1.8)	24.9 (1.4)	24.4 (2.3)	0.019
Biochemical data				
Serum creatinine, µmol/L	85.9 (14.9)	84.9 (12.6)	87.1 (13.3)	0.24
eGFR, mL/min/1.73 m ²	81.6 (16.5)	82.1 (14.8)	89.1 (18.0)	<0.0001
Plasma glucose, mmol/L	4.98 (0.78)	4.94 (0.57)	4.78 (0.41)	0.0010
Total serum cholesterol, mmol/L	5.24 (0.94)	5.43 (0.98)	5.11 (0.96)	0.0018
HDL serum cholesterol, mmol/L	1.41 (0.34)	1.47 (0.38)	1.43 (0.34)	0.19
Total-to-HDL serum cholesterol ratio	3.90 (1.03)	3.89 (1.00)	3.72 (0.97)	0.12
dpucMGP, µg/L	4.86 (3.48)	5.09 (4.47)	4.54 (2.32)	0.25
Serum γ-glutamyltransferase, U/L	22.0 (16.0–35.0)	21.0 (14.0–32.0)	22.0 (15.0–31.0)	0.53
Air pollutants				
PM ₁₀ , µg/m ³	15.7 (0.64)	17.3 (0.77)	20.9 (1.02)	—
PM _{2.5} , µg/m ³	12.1 (0.24)	12.7 (0.36)	14.1 (0.52)	—
BC, µg/m ³	0.56 (0.06)	0.69 (0.08)	0.96 (0.11)	—
NO ₂ , µg/m ³	14.6 (1.12)	15.8 (1.55)	21.0 (2.87)	—

Note: To convert dpucMGP from µg/L into pmol/L, multiply by 94.299. Smoking was the current use of any smoking materials on a daily basis. Socioeconomic status was coded according to the UK Office of Population Censuses and Surveys and simplified into a linear scale with scores ranging from 1 to 3 showing increasing affluence. Hypertension was a blood pressure of ≥ 140 mm Hg systolic or ≥ 90 mm Hg diastolic or use of antihypertensive drugs. Diabetes was a fasting plasma glucose of ≥ 7.0 mmol/L, a self-reported diagnosis, diabetes documented in practice or hospital records, or use of antidiabetic drugs. γ-Glutamyltransferase was measured as index of alcohol intake and logarithmically transformed and presented as geometric mean (IQR). *p*-Values are for linear trend across the thirds of the distribution of averaged annual (2010–2014) PM₁₀ levels. — indicates that given the high correlation between the air pollutants (Table S2), the trend *p*-value was not computed. BC, black carbon; dpucMGP, desphospho-uncarboxylated matrix Gla protein; eGFR, glomerular filtration rate derived from serum creatinine, using the Chronic Kidney Disease Epidemiology Collaboration equation; FLEMENGHO, Flemish Study on Environment, Genes, and Health Outcomes; NA, not applicable; HDL, high-density lipoprotein; IQR, interquartile range; NO₂, nitrogen dioxide; PM_{2.5}, particulate matter with aerodynamic diameter ≤ 2.5 µm; PM₁₀, particulate matter with aerodynamic diameter ≤ 10 µm; UPP-age, urinary peptidomic profile age; UPP-age-R, residual of the regression of UPP-age on chronological age.

dpucMGP as Effect Modifier

Risk factors were aggregated into five categories reflecting their target operability: the vasculature, the kidney, glucose and lipid

metabolism, and inflammation. The correlation matrix, including the individual and aggregated risk factors, is summarized in Figure S5. Of the 18 individual (Table S6) and the 5 aggregated (Table S7) risk factors, only dpucMGP significantly and consistently affected

Table 2. Association of UPP-age-R with an IQR higher level of air pollutants in 660 FLEMENGHO participants.

Air pollutant (+IQR)	Unadjusted		Adjusted	
	Estimate (95% CI)	<i>p</i> -Value	Estimate (95% CI)	<i>p</i> -Value
PM ₁₀ (+3.79 µg/m ³)	1.06 (0.12, 2.01)	0.027	1.04 (0.11, 1.98)	0.029
PM _{2.5} (+1.59 µg/m ³)	1.21 (0.19, 2.23)	0.019	1.17 (0.16, 2.18)	0.023
BC (+0.31 µg/m ³)	1.07 (0.11, 2.02)	0.029	1.02 (0.08, 1.97)	0.034
NO ₂ (+5.25 µg/m ³)	0.88 (0.01, 1.76)	0.049	0.87 (−0.01, 1.74)	0.051

Note: Estimates, given as difference in UPP-age-R (in years) with 95% CI, were derived by mixed models that accounted for clustering between participants sharing the same residential address as random effect. Unadjusted models did not account for other variables. Adjusted models additionally accounted for sex, age, body mass index, mean arterial pressure, plasma glucose, γ-glutamyltransferase, current smoking, the total-to-high-density lipoprotein serum cholesterol ratio, glomerular filtration rate, and socioeconomic status as fixed effects. BC, black carbon; CI, confidence interval; FLEMENGHO, Flemish Study on Environment, Genes, and Health Outcomes; IQR, interquartile range; NO₂, nitrogen dioxide; PM_{2.5}, particulate matter with aerodynamic diameter ≤ 2.5 µm; PM₁₀, particulate matter with aerodynamic diameter ≤ 10 µm; UPP-age, urinary peptidomic profile age; UPP-age-R, residual of the regression of UPP-age on chronological age.

the multivariable-adjusted association between UPP-age-R and the four air pollutants, with higher dpucMGP showing stronger associations of air pollutants and UPP-age-R. The linear interaction terms between dpucMGP and the air pollutant were significant with p -values of 0.0032 for PM₁₀, 0.0075 for PM_{2.5}, 0.012 for BC, and 0.0074 for NO₂. The Spearman rank correlation coefficients of dpucMGP with the air pollutants were not significant: -0.027 ($p = 0.54$) for PM₁₀; -0.034 ($p = 0.38$) for PM_{2.5}; -0.032 for BC; and -0.016 ($p = 0.68$) for NO₂.

The combined contribution of the air pollutants and dpucMGP to UPP-age-R was therefore investigated in multivariable-adjusted analyses of the whole study population and in similarly adjusted analyses stratified by median dpucMGP (4.26 $\mu\text{g/L}$). First, in the whole study population, UPP-age-R tended to be higher with both air pollutants and dpucMGP (Figure 1). Second, individuals with high dpucMGP (above 4.26 $\mu\text{g/L}$) in comparison with low dpucMGP had a substantially higher risk profile (Table S8), and in these participants an IQR higher level in the air pollutants was associated with a higher UPP-age-R of 2.03 (95% CI: 0.60, 3.46; $p = 0.0062$), 2.22 (95% CI: 0.71, 3.74; $p = 0.0048$), 2.00 (95% CI: 0.56, 3.43; $p = 0.0073$), and 2.09 (95% CI: 0.77, 3.41; $p = 0.0024$) y for PM₁₀, PM_{2.5}, BC, and NO₂, respectively (Figure 2). In contrast, if dpucMGP was <4.26 $\mu\text{g/L}$ (Figure 2), no association between air pollution and UPP-age-R was observed ($p \geq 0.43$).

The geocorrelation coefficients between UPP-age-R and the air pollutants at the individual level or aggregated by municipality are listed in Table S9 for the whole study population and for individuals stratified by the median dpucMGP level. In analyses including the participants with dpucMGP of 4.26 $\mu\text{g/L}$ or higher ($n = 330$), the geocorrelations of multivariable-adjusted UPP-age-R with PM₁₀, PM_{2.5}, BC, and NO₂, were 0.155 ($p = 0.0048$), 0.159 ($p = 0.0036$), 0.151 ($p = 0.0061$), and 0.168 ($p = 0.0022$), respectively (Table S9

and Figure S6); the corresponding correlation coefficients at the aggregate level (Table S9 and Figure S7) were 0.721 ($p = 0.023$), 0.636 ($p = 0.054$), 0.697 ($p = 0.031$), and 0.600 ($p = 0.073$).

In sensitivity analyses (Table S10), we analyzed the robustness of the associations between UPP-age-R and the different air pollutants in participants with high dpucMGP. Confirmatory associations were observed between UPP-age-R and the air pollutants in men and women, in models excluding patients on treatment with coumarins or having diabetes, or excluding current smokers, or in models in which annual income averaged per statistical sector was added as explanatory covariable.

Mediation Analysis

The median follow-up of the whole cohort amounted to 12.4 y (IQR: 10.7–13.1 y; 10th–90th percentile interval: 10.1–13.7 y) with the number of follow-up years being slightly higher (Wilcoxon p -value: 0.024) among participants with dpucMGP below 4.26 $\mu\text{g/L}$ [median: 12.4 y (IQR: 10.7–13.2 y); total number of person-years: 3,961] than in those with dpucMGP levels of 4.26 $\mu\text{g/L}$ or higher [12.2 y (IQR: 10.7–13.1 y); total number of person-years: 3,853]. The number of deaths occurring during follow-up was 11/330 (3.3%) and 4/330 (1.2%) due to cardiovascular disease in the low dpucMGP group and 38/330 (11.5%) and 15/330 (4.6%), respectively, in the high dpucMGP group.

The multivariable-adjusted hazard ratios, relating mortality to a 10-y higher UPP-age-R in the whole cohort were 1.84 (95% CI: 1.21, 2.73; $p = 0.0042$) for total mortality and 2.23 (95% CI: 1.20, 4.13; $p = 0.0011$) for cardiovascular mortality. Whether UPP-age-R mediated the association between total and cardiovascular mortality and the air pollutants was examined in a mediation analysis stratified by the median dpucMGP group (Table

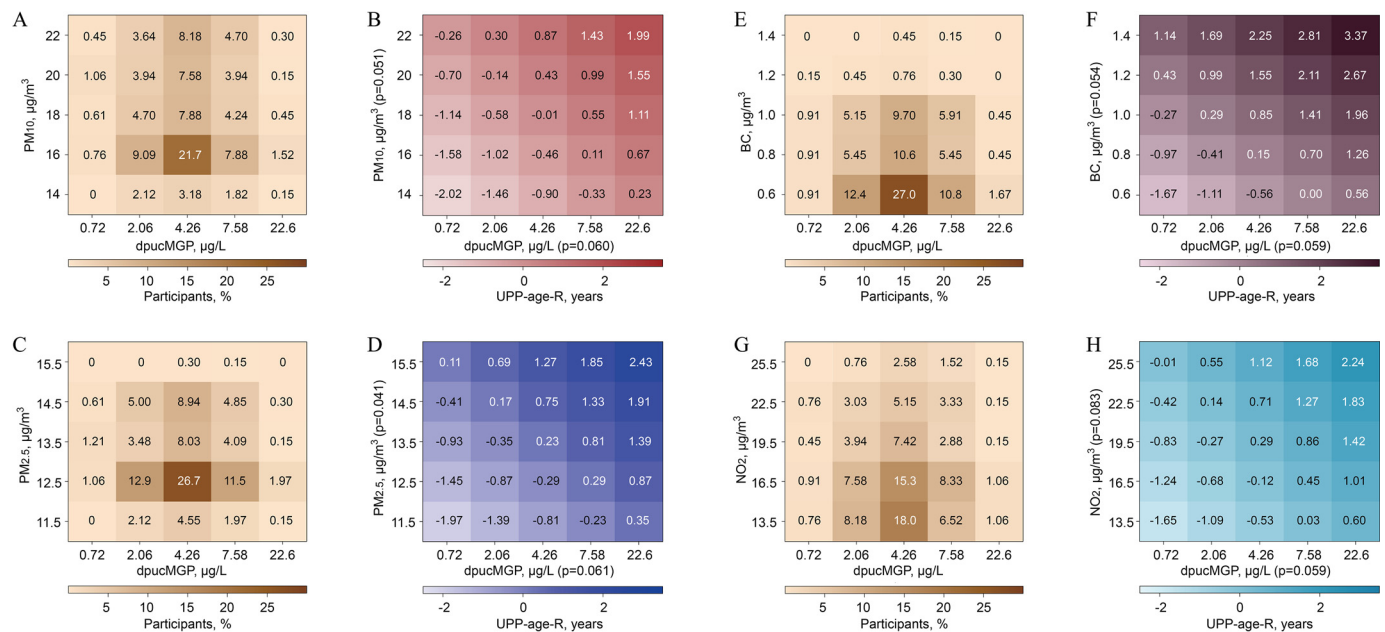


Figure 1. Heat maps showing the difference in UPP-age-R associated with the combined contributions of the air pollutants and dpucMGP in 660 FLEMENGHO participants. Differences in UPP-age-R were derived by mixed models, which included both the air pollutants and dpucMGP as independent variables. All models accounted for clustering between participants sharing the same residential address as random effect and for sex, age, body mass index, mean arterial pressure, plasma glucose, γ -glutamyltransferase, current smoking, the total-to-high-density lipoprotein serum cholesterol ratio, glomerular filtration rate, and socioeconomic status as fixed effects. Panels (A), (C), (E), and (G) provide the percentage of study participants ($n = 660$ in total) in each box of the cross-classification between dpucMGP, plotted along the horizontal axis and the air pollutant plotted along the vertical axis. Panels (B), (D), (F), and (H) show changes in UPP-age-R (in years) in association with dpucMGP and PM₁₀ (B), PM_{2.5} (D), BC (F) and NO₂ (H) concentrations. p -Values represent the significance of the linear associations between the air pollutant or dpucMGP with UPP-age-R in full adjusted models. Note: BC, black carbon; dpucMGP, desphospho-uncarboxylated matrix Gla protein; FLEMENGHO, Flemish Study on Environment, Genes, and Health Outcomes; NO₂, nitrogen dioxide; PM_{2.5}, particulate matter with aerodynamic diameter ≤ 2.5 μm ; PM₁₀, particulate matter with aerodynamic diameter ≤ 10 μm ; UPP-age, urinary peptidomic profile age; UPP-age-R, residual of the regression of UPP-age on chronological age.

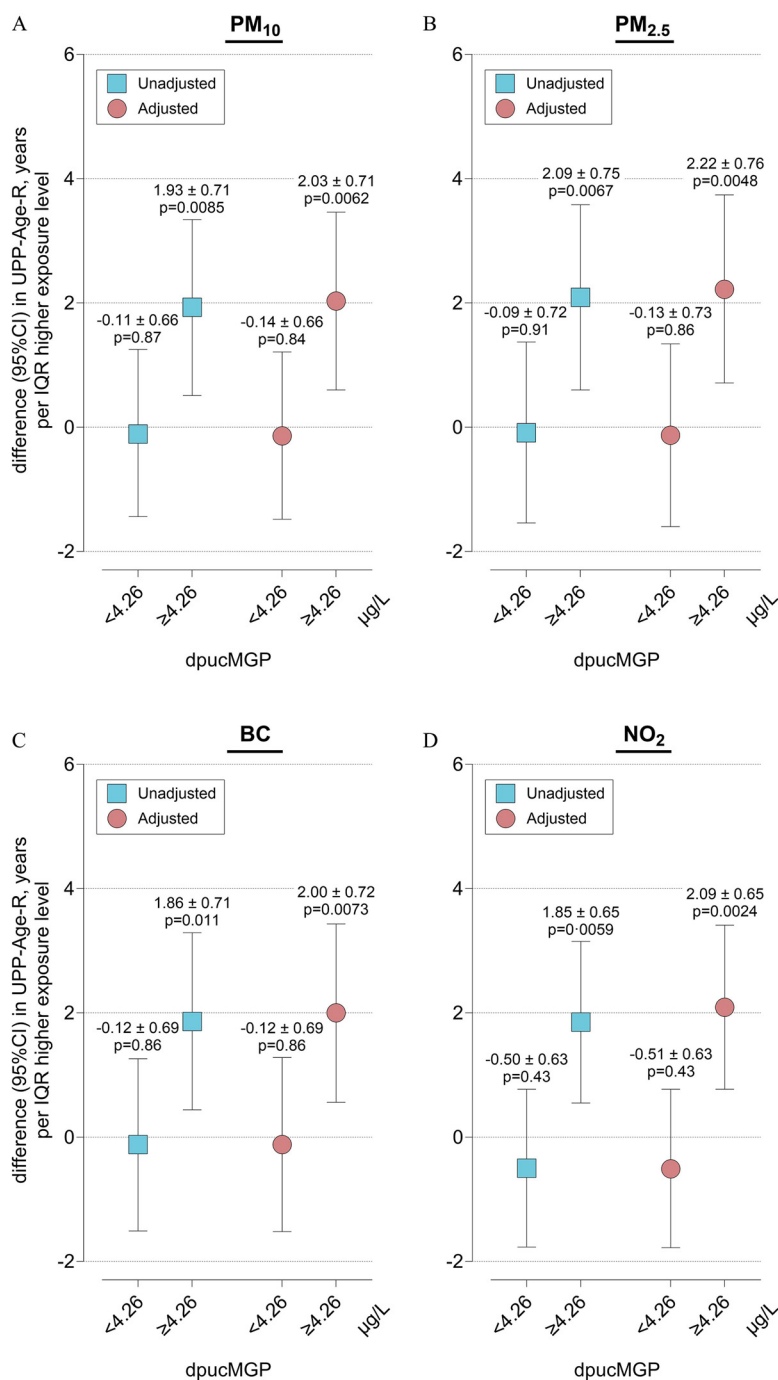


Figure 2. Association of UPP-age-R with air pollutants in 660 FLEMENGHO participants stratified by the median (4.26 µg/L) level of dpucMGP. Red squares are unadjusted estimates with 95% CI bars. Blue circles are adjusted estimates with 95% CI bars and were derived by mixed models, which accounted for clustering between participants sharing the same residential address as random effect and for sex, age, body mass index, mean arterial pressure, plasma glucose, γ -glutamyltransferase, current smoking, the total- to high-density lipoprotein serum cholesterol ratio, glomerular filtration rate, and socioeconomic status as fixed effects. Estimates provided as a difference in UPP-age-R (in years) for an IQR higher level in PM₁₀ [$+3.79 \mu\text{g}/\text{m}^3$, (A)]; PM_{2.5} [$+1.59 \mu\text{g}/\text{m}^3$, (B)]; BC [$+0.31 \mu\text{g}/\text{m}^3$, (C)]; and NO₂ [$+5.25 \mu\text{g}/\text{m}^3$, (D)]. Numerical estimates are provided with \pm SE and *p*-value. *n* = 330 for dpucMGP <4.26 µg/L and *n* = 330 for dpucMGP \geq 4.26 µg/L. Note: BC, black carbon; CI, confidence interval; dpucMGP, desphospho-uncarboxylated matrix Gla protein; FLEMENGHO, Flemish Study on Environment, Genes, and Health Outcomes; IQR, interquartile range; NO₂, nitrogen dioxide; PM_{2.5}, particulate matter with aerodynamic diameter $\leq 2.5 \mu\text{m}$; PM₁₀, particulate matter with aerodynamic diameter $\leq 10 \mu\text{m}$; SE, standard error; UPP-age, urinary peptidomic profile age; UPP-age-R, residual of the regression of UPP-age on chronological age.

S11), which is summarized in Figure 3. In participants with dpucMGP levels below 4.26 µg/L, none of the hazard ratios modeling the indirect (via UPP-age-R) and direct associations between total mortality and the air pollutants reached significance (Table S11). In participants with dpucMGP levels of 4.26 µg/L

or higher, UPP-age-R was an indirect mediator of the associations of total and cardiovascular mortality with the air pollutants with indirect multivariable-adjusted hazard ratios of ranging from 1.107 (95% CI: 1.002, 1.222; *p* = 0.045), 1.107 (95% CI: 1.004, 1.221; *p* = 0.041), 1.094 (95% CI: 1.000, 1.196; *p* = 0.049), 1.110

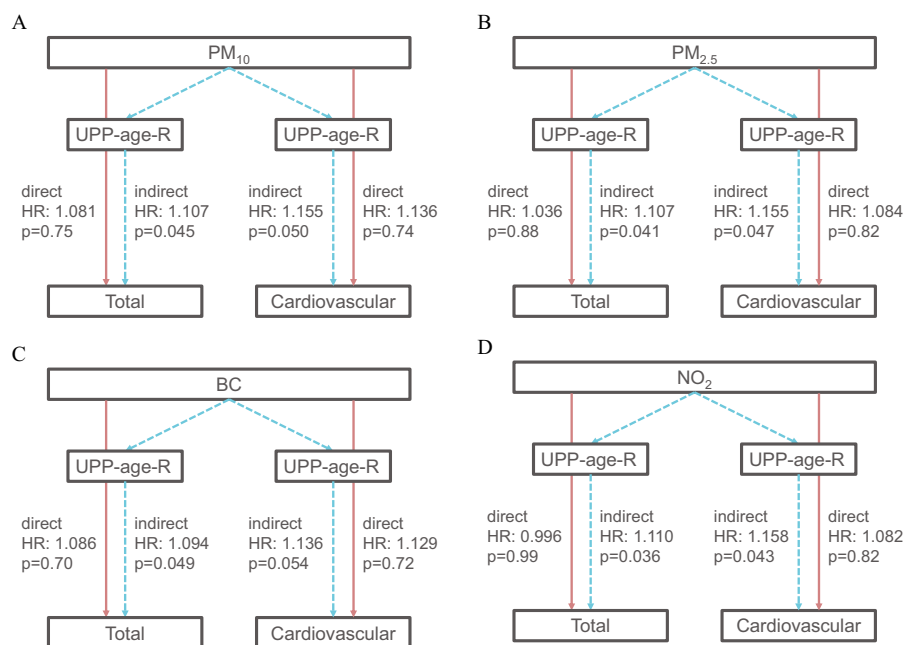


Figure 3. Estimated direct and indirect (via UPP-age-R) effects of air pollutant exposure on total and cardiovascular mortality in 330 FLEMENGHO participants with dpucMGP of 4.26 $\mu\text{g}/\text{L}$ (median) or higher. Multivariable-adjusted HRs with corresponding *p*-values were calculated by Cox proportional hazards regression. Models accounted for sex, age, body mass index, mean arterial pressure, the total-to-high-density-lipoprotein cholesterol ratio, plasma glucose, γ -glutamyltransferase, current smoking, glomerular filtration rate, and socioeconomic status. HRs express the relative risk for a IQR higher level in PM₁₀ [$+3.79 \mu\text{g}/\text{m}^3$, (A)]; PM_{2.5} [$+1.59 \mu\text{g}/\text{m}^3$, (B)], BC [$+0.31 \mu\text{g}/\text{m}^3$, (C)]; and NO₂ [$+5.25 \mu\text{g}/\text{m}^3$, (D)]. The incidence of total and cardiovascular mortality amounted to 38/330 (11.5%) and 15/330 (4.5%), respectively. Note: BC, black carbon; dpucMGP, desphospho-uncarboxylated matrix Gla protein; FLEMENGHO, Flemish Study on Environment, Genes, and Health Outcomes; HR, hazard ratio; NO₂, nitrogen dioxide; PM_{2.5}, particulate matter with aerodynamic diameter $\leq 2.5 \mu\text{m}$; PM₁₀, particulate matter with aerodynamic diameter $\leq 10 \mu\text{m}$; UPP-age, urinary peptidomic profile age; UPP-age-R, residual of the regression of UPP-age on chronological age.

(95% CI: 1.007, 1.224; $p = 0.036$) for PM₁₀, PM_{2.5}, BC, and NO₂, respectively. For cardiovascular mortality the corresponding indirect multivariable-adjusted hazard ratios were 1.155 (95% CI: 1.000, 1.335; $p = 0.050$), 1.155 (95% CI: 1.002, 1.332; $p = 0.047$), 1.136 (95% CI: 0.998, 1.294; $p = 0.054$), 1.158 (95% CI: 1.005, 1.335; $p = 0.043$) for PM₁₀, PM_{2.5}, BC, and NO₂, respectively (Figure 3 and Table S11). In the high dpucMGP stratum, none of the hazard ratios reflecting a direct association of total and cardiovascular mortality with the air pollutants were observed (Figure 3; Table S11).

Discussion

UPP-age-R is a urinary peptidomic biomarker, which has been developed in FLEMENGHO and which has been extensively validated in population and patient cohorts.¹³ Independent of chronological age, UPP-age-R predicted total and cardiovascular mortality. The primary novel finding of the current study is that UPP-age-R is positively associated with airborne pollutants including PM₁₀, PM_{2.5}, BC, and NO₂, and that these associations are stronger in participants with poor vitamin K status, as captured by a high plasma dpucMGP level. The correlations between UPP-age-R per each individual's residential address and airborne exposure were all ≥ 0.151 ($p = 0.0061$). In participants with a high plasma dpucMGP, the multivariable-adjusted associations of total and cardiovascular mortality with the air pollutants were indirectly mediated via UPP-age-R, whereas the direct associations were not significant.

To the best of our knowledge, the current study is the first to examine the relation between accelerated aging and exposure to airborne particulate using a UPP-derived biomarker (UPP-age-R). The present observations are in line with other studies based on epigenetic aging clocks.^{38–41} In the German KORA F4 study (mean

age: 61 y), an IQR (0.97 $\mu\text{g}/\text{m}^3$) increment in ambient PM_{2.5} was associated with an increase of 0.32 to 0.35 y in an epigenetic aging clock (Horvath clock).³⁸ In the Lothian Birth Cohort, the corresponding estimate was $+0.299$ y per $\mu\text{g}/\text{m}^3$ in PM_{2.5}.⁴² In the Normative Aging Study,^{39,41} PM_{2.5} exposure was associated with a 0.64-y increment in Horvath aging clock per 2.16 $\mu\text{g}/\text{m}^3$ (IQR) increment in exposure. In comparison with the epigenetic approaches, UPP-age-R is noninvasive and easily administrable, because it only requires a midmorning urine sample without the need for blood sampling and involves the measurement of 20,000 omics signals, much less than the 0.5–1.0 million signals making up epigenetic markers. In addition, peptides are more strongly related to clinical phenotypes in comparison with upstream epigenetic signals, which provide a more straightforward biological interpretation of underlying, and potentially targetable, pathways in health and disease.

From a mechanistic point of view, inhaled particles can cause not only local inflammation of the airways and alveoli, but also systemwide a chronic low-grade inflammatory state as a result of “a spillover effect” and via the circulation of nano-sized particles.^{3,5} This effect might cause accelerated biological aging as captured here by a higher UPP-age-R. PM generates reactive oxygen species (ROS), either directly by ROS formation on the particle surface via Fenton reactions or indirectly through altered functions of NADPH-oxidases, mitochondria, and activation of inflammatory responses via the release of proinflammatory mediators [TNF- α , interleukin-6 (IL-6), and interleukin-1 β (IL-1 β)] by alveolar macrophages.^{43–45} The concept that air pollutants can cause systemic inflammation is further supported by experimental studies reporting higher expression of NF- κ B, the key inflammation mediator, which induces the expression of pro-inflammatory genes.^{46,47} Over an individual's lifetime, long-term exposure to

airborne PM probably contributes to “inflammaging,”⁴⁸ characterized by an increase in blood inflammatory markers reflective of a chronic low-grade inflammation, which in turn entails a higher risk for chronic morbidities, disabilities, frailty, and premature death.⁴⁹

The observation that high dpucMGP levels (reflecting poor vitamin K status) steepens the relation between UPP-age-R and the air pollutants is novel but not surprising, given a large body of available evidence. Vitamin K-dependent proteins (VKDPs) include hepatic VKDPs, which are mainly involved in blood coagulation, and extrahepatic VKDPs, which have numerous functions related to the high affinity of their Gla residues for calcium. The extrahepatic VKDP osteocalcin regulates bone formation and mineralization.⁵⁰ Vascular smooth muscle cells and the endothelium synthesize a small secretory protein (11 kD), which is named MGP (matrix Gla protein) because it contains five γ -carboxyglutamate (Gla) amino acid residues. Activation of MGP by vascular stress or other stimuli requires two posttranslational modifications: serine phosphorylation and vitamin K-dependent γ -glutamate carboxylation.⁵¹ Activated MGP is a multifaceted protector of the micro- and macrovasculature, renal function, and tissue integrity.¹⁸ In the current study, poor vitamin K status was associated with a substantially elevated risk factor load and higher UPP-age-R (Table S8). In FLEMENGHO, higher dpucMGP predicted total, noncancer, and cardiovascular mortality, but lower coronary risk.¹⁴ A Mendelian randomization analysis, using functional variants of the MGP gene as instrumental variables, suggested causality for the associations with noncancer mortality and coronary events.¹⁴

Strengths and Limitations

This study has strong points. UPP-age-R has been replicated and validated for its association with risk factors, the intensity of drug treatment to control risk factors, and the incidence of mortality and adverse health outcomes.¹³ Nevertheless, UPP-age-R might be more dynamic in comparison with epigenetic-derived clocks, because it is closely related to the clinical phenotype and might be dysregulated in severe disease phenotypes. In addition, the UPP-age-R is currently further limited in its wide application in comparison with epigenetic BeadChip-derived aging clocks because it depends on the specific presented CE-MS methodology. FLEMENGHO is a long-term study (Figure S1) with random sampling of the population from a geographically defined area in northern Belgium (Figure S2) and is therefore representative of western European countries. Furthermore, each individual's exposure to airborne PM was estimated, using a high-resolution spatiotemporal interpolation method. Obviously, the current study must also be interpreted in the context of its limitations. First, UPP-age-R (2005–2010) was measured prior to the air pollution data (2010–2014). However, studies conducted in the Netherlands,²⁹ Italy,^{30,33} Canada,³¹ and the United Kingdom³² demonstrated that the land-use models applied in the current study are representative of long-term air pollution exposure for periods of 10 y or longer prior to the actual modeling and that spatial contrasts in air pollution do not substantially change over time.^{29–33} Second, being an observational cohort study, FLEMENGHO was not designed to unravel the molecular mechanism underlying the associations between UPP-age-R and the airborne particulate. Third, this study, using a modest sample size, shows the potential protective effects of vitamin K in the general population; however, these findings should be further externally confirmed using independent and large population-based studies. In addition, this study cannot prove causality for the protective effects of vitamin K, which should be elucidated using *in vitro* and *in vivo* experimental models. Nevertheless, we show that participants with a poor vitamin K status have a higher risk profile and appear to be more susceptible to the air pollution–

induced molecular aging effects. In addition, due to the rather small study area, we observed high correlations between the different air pollutants and a lower variation within exposure levels, partly explaining similar and consistent findings for the different pollutants used. This high correlation between air pollutants made it impossible in the current study to construct a multipollutant model to unravel independent or combined exposure effects. Finally, whereas by definition UPP-age-R is independent of calendar age, dpucMGP increases with chronological age,¹⁸ raising the possibility that advancing age might explain the effect modification picked up by dpucMGP. However, in the derivation of UPP-age-R as function of air pollution, the observed interaction between vitamin K status and exposure to airborne pollutants was independent of age.

Public Health Implications

High levels of plasma dpucMGP are a proxy for vitamin K deficiency, in FLEMENGHO levels ranging from ~ 1.4 to ~ 4.6 $\mu\text{g/L}$ (~ 130 to ~ 437 pmol/L), were optimal in terms of the risk for mortality and cardiovascular disease,¹⁴ and the 4.6- $\mu\text{g/L}$ threshold corresponded with 63rd percentile of dpucMGP distribution. DpucMGP increases with age,¹⁸ and other causes of a high dpucMGP include intestinal diseases negatively affecting the gut microflora and poor nutrition, in particular in the deprived segments of the population. However, which levels of plasma dpucMGP should be acted on for optimal health remains an issue to be resolved.¹⁸ Given the worldwide demographic transition with growing longevity¹ and given that exposure to airborne pollutants is currently the predominant environmental risk factor,² vitamin K supplementation might be recommended among the lifestyle measures promoting healthy aging. Dietary sources of vitamin K include leafy vegetables (phylloquinone; vitamin K1) and fermented foods (menaquinones; vitamin K2), such as cheese and soybeans fermented with *Bacillus subtilis* var. natto (natto).⁵² In humans, gut bacteria also produce vitamin K.⁵³ In contrast to dietary vitamins, which are absorbed in the proximal tract of the small intestine, the predominant uptake of microbiotically synthesized vitamins occurs in the colon.⁵⁴ Abuse of antibiotics impairs the synthesis of vitamin K by the gut flora. There is currently no evidence from randomized trials, for instance with cluster randomization of geographical units with similar exposure to airborne PM, to support this recommendation. However, vitamin K has desired anti-inflammatory properties⁵⁵ via suppressing NF κ B/NRF signaling,⁵⁶ prevention of lipid peroxidation,⁵⁷ glutathione depletion-induced oxidative cell death,⁵⁸ and other mechanisms.⁵⁹

Conclusions

Ambient air pollution is associated with accelerated aging as reflected by the urinary peptidome (UPP-age-R), high vitamin K status having a potential protective effect. Furthermore, in participants with a high dpucMGP, reflecting poor vitamin K, mediation analysis showed total and cardiovascular mortality to be associated with air pollutants via UPP-age-R. Current guidelines to decrease the adverse health effects associated with airborne PM might include advice on protective effect modifiers, such as vitamin K intake. Regulators, such as the World Health Organization, may advise, in addition to tightening acceptable exposure to air pollutants, lifestyle changes to decrease vitamin K deficiency, which affects over one-third of Europeans and perhaps higher proportions in non-European populations.⁶⁰

Acknowledgments

FLEMENGHO was supported by the European Union (grants IC15-CT98-0329-EPOGH, LSHM CT 037093-InGenious

HyperCare, HEALTH-201550-HyperGenes, HEALTH-278249-EU-MASCARA, HEALTH-305507 HOMAGE), the European Research Council (Advanced Researcher Grant-2011-294713-EPLORE and Proof-of-Concept Grant-713601 uPROPHET), the European Research Area Net for Cardiovascular Diseases (JTC2017-046-PROACT), and the Research Foundation Flanders, Ministry of the Flemish Community, Brussels, Belgium. APPREMED (www.appremed.org) received a nonbinding grant from OMRON Healthcare Co., Ltd., Kyoto, Japan. Dries Martens holds a postdoctoral grant by the Research Foundations Flanders (FWO grants 12X9620N and 12X9623N). Ana Inês Silva has received funding from the European Union's Horizon 2020 Research and Innovation Programme under grant agreement no. 956780.

D.S.M., T.S.N., and J.A.S. conceptualized the study. H.M. and A.L. did the proteomic urine analyses. A.I.S. performed the geographical analyses and constructed the air pollution charts. D.-W.A., Y.-L.Y., F.F.W., K.S.S., M.R., and J.A.S. maintained the FLEMENGHO database. D.S.M., Y.-L.Y., C.W., and J.A.S. did the statistical analysis. D.S.M. and J.A.S. wrote the first draft of the manuscript. D.S.M. and J.A.S. had access to and verified the data reported in this study. All authors interpreted the results, commented on successive drafts of the manuscript and approved the final version.

Anonymized participant data will be made available on request directed to the corresponding author. Proposals will be reviewed and approved by the authors with scientific merit and feasibility as the criteria. After approval of a proposal, data can be shared via a secure online platform after signing a data access and confidentiality agreement. Data will be made available for a maximum of 5 y after a data sharing agreement has been signed.

References

- Wang H, Abbas KM, Abbasifard M, Abbasi-Kangevari M, Abbastabar H, Abd-Allah F, et al. 2020. Global age-sex-specific fertility, mortality, healthy life expectancy (HALE), and population estimates in 204 countries and territories, 1950–2019: a comprehensive demographic analysis for the Global Burden of Disease Study 2019. *Lancet* 396(10258):1160–1203, PMID: 33069325, [https://doi.org/10.1016/S0140-6736\(20\)30977-6](https://doi.org/10.1016/S0140-6736(20)30977-6).
- Murray CJL, Aravkin AY, Zheng P, Abbafati C, Abbas KM, Abbasi-Kangevari M, et al. 2020. Global burden of 87 risk factors in 204 countries and territories, 1990–2019: a systematic analysis for the Global Burden of Disease Study 2019. *Lancet* 396(10258):1223–1249, PMID: 33069327, [https://doi.org/10.1016/S0140-6736\(20\)30752-2](https://doi.org/10.1016/S0140-6736(20)30752-2).
- Nemmar A, Hoet PHM, Vanquickenborne B, Dinsdale D, Thomeer M, Hoylaerts MF, et al. 2002. Passage of inhaled particles into the blood circulation in humans. *Circulation* 105(4):411–414, PMID: 11815420, <https://doi.org/10.1161/hc0402.104118>.
- Bongaerts E, Mamiã K, Rooda I, Björvang RD, Papaikonomou K, Gidlöf SB, et al. 2023. Ambient black carbon particles in human ovarian tissue and follicular fluid. *Environ Int* 179:108141, PMID: 37603992, <https://doi.org/10.1016/j.envint.2023.108141>.
- Bongaerts E, Lecante LL, Bove H, Roeflaers MJB, Ameloot M, Fowler PA, et al. 2022. Maternal exposure to ambient black carbon particles and their presence in maternal and fetal circulation and organs: an analysis of two independent population-based observational studies. *Lancet Planet Health* 6(10):e804–e811, PMID: 36208643, [https://doi.org/10.1016/S2542-5196\(22\)00200-5](https://doi.org/10.1016/S2542-5196(22)00200-5).
- López-Otín C, Blasco MA, Partridge L, Serrano M, Kroemer G. 2023. Hallmarks of aging: an expanding universe. *Cell* 186(2):243–278, PMID: 36599349, <https://doi.org/10.1016/j.cell.2022.11.001>.
- Peters A, Nawrot TS, Baccarelli AA. 2021. Hallmarks of environmental insults. *Cell* 184(6):1455–1468, PMID: 33657411, <https://doi.org/10.1016/j.cell.2021.01.043>.
- Hahad O, Frenis K, Kuntic M, Daiber A, Münzel T. 2021. Accelerated aging and age-related diseases (CVD and neurological) due to air pollution and traffic noise exposure. *Int J Mol Sci* 22(5):2419, PMID: 33670865, <https://doi.org/10.3390/ijms22052419>.
- Martens DS, Cox B, Janssen BG, Clemente DBP, Gasparrini A, Vanpoucke C, et al. 2017. Prenatal air pollution and newborns' predisposition to accelerated biological aging. *JAMA Pediatr* 171(12):1160–1167, PMID: 29049509, <https://doi.org/10.1001/jamapediatrics.2017.3024>.
- Pieters N, Janssen BG, Dewitte H, Cox B, Cuyppers A, Lefebvre W, et al. 2016. Biomolecular markers within the core axis of aging and particulate air pollution exposure in the elderly: a cross-sectional study. *Environ Health Perspect* 124(7):943–950, PMID: 26672058, <https://doi.org/10.1289/ehp.1509728>.
- White AJ, Kresovich JK, Keller JP, Xu Z, Kaufman JD, Weinberg CR, et al. 2019. Air pollution, particulate matter composition and methylation-based biologic age. *Environ Int* 132:105071, PMID: 31387022, <https://doi.org/10.1016/j.envint.2019.105071>.
- Klein J, Papadopoulos T, Mischak H, Mullen W. 2014. Comparison of CE-MS/MS and LC-MS/MS sequencing demonstrates significant complementarity in natural peptide identification in human urine. *Electrophoresis* 35(7):1060–1064, PMID: 24254231, <https://doi.org/10.1002/elps.201300327>.
- Martens DS, Thijs L, Latosinska A, Trenson S, Siwy J, Zhang Z-Y, et al. 2021. Urinary peptidomic profiles to address age-related disabilities: a prospective population study. *Lancet Healthy Longev* 2(11):e690–e703, PMID: 34766101, [https://doi.org/10.1016/S2666-7568\(21\)00226-9](https://doi.org/10.1016/S2666-7568(21)00226-9).
- Liu Y-P, Gu Y-M, Thijs L, Knapen MHJ, Salvi E, Citterio L, et al. 2015. Inelative matrix Gla protein is causally related to adverse health outcomes: a Mendelian randomization study in a Flemish population. *Hypertension* 65(2):463–470, PMID: 25421980, <https://doi.org/10.1161/HYPERTENSIONAHA.114.04494>.
- Myers GL, Miller WG, Coresh J, Fleming J, Greenberg N, Greene T, et al. 2006. Recommendations for improving serum creatinine measurement: a report from the laboratory working group of the national kidney disease education program. *Clin Chem* 52(1):5–18, PMID: 16332993, <https://doi.org/10.1373/clinchem.2005.0525144>.
- Levey AS, Stevens LA, Schmid CH, Zhang YL, Castro AF, Feldman HI, et al. 2009. A new equation to estimate glomerular filtration rate. *Ann Intern Med* 150(9):604–612, PMID: 19414839, <https://doi.org/10.7326/0003-4819-150-9-200905050-00006>.
- Matthews DR, Hosker JP, Rudenski AS, Naylor BA, Treacher DF, Turner RC. 1985. Homeostasis model assessment: insulin resistance and beta-cell function from fasting plasma glucose and insulin concentrations in man. *Diabetologia* 28(7):412–419, PMID: 3899825, <https://doi.org/10.1007/BF00280883>.
- Wei FF, Trenson S, Verhamme P, Vermeer C, Staessen JA. 2019. Vitamin K-dependent matrix Gla protein as multifaceted protector of vascular and tissue integrity. *Hypertension* 73(6):1160–1169, PMID: 31006332, <https://doi.org/10.1161/HYPERTENSIONAHA.119.12412>.
- Office of Population Census and Surveys. 1980. Classification of Occupations and Coding Index. London, UK: Governmental Statistical Service.
- Staessen JA, Fagard R, Amery A. 1994. Life style as a determinant of blood pressure in the general population. *Am J Hypertens* 7(8):685–694, PMID: 7986458, <https://doi.org/10.1093/ajh/7.8.685>.
- Mischak H, Vlahou A, Ioannidis JP. 2013. Technical aspects and inter-laboratory variability in native peptide profiling: the CE-MS experience. *Clin Biochem* 46(6):432–443, PMID: 23041249, <https://doi.org/10.1016/j.clinbiochem.2012.09.025>.
- Latosinska A, Siwy J, Mischak H, Frantzi M. 2019. Peptidomics and proteomics based on CE-MS as a robust tool in clinical application: the past, the present, and the future. *Electrophoresis* 40(18–19):2294–2308, PMID: 31054149, <https://doi.org/10.1002/elps.201900091>.
- Jantos-Siwy J, Schiffer E, Brand K, Schumann G, Rossing K, Delles C, et al. 2009. Quantitative urinary proteome analysis for biomarker evaluation in chronic kidney disease. *J Proteome Res* 8(1):268–281, PMID: 19012428, <https://doi.org/10.1021/pr800401m>.
- Mavrogeorgis E, Mischak H, Latosinska A, Siwy J, Jankowski V, Jankowski J. 2021. Reproducibility evaluation of urinary peptide detection using CE-MS. *Molecules* 26(23):7260, PMID: 34885840, <https://doi.org/10.3390/molecules26237260>.
- Zürbig P, Renfrow MB, Schiffer E, Novak J, Walden M, Wittke S, et al. 2006. Biomarker discovery by CE-MS enables sequence analysis via MS/MS with platform-independent separation. *Electrophoresis* 27(11):2111–2125, PMID: 16645980, <https://doi.org/10.1002/elps.200500827>.
- Janssen S, Dumont G, Fierens F, Mensink C. 2008. Spatial interpolation of air pollution measurements using CORINE land cover data. *Atmospheric Environment* 42(20):4884–4903, <https://doi.org/10.1016/j.atmosenv.2008.02.043>.
- Lefebvre W, Degrawe B, Beckx C, Vanhulsel M, Kochan B, Bellemans T, et al. 2013. Presentation and evaluation of an integrated model chain to respond to traffic- and health-related policy questions. *Environ Model Softw* 40(0):160–170, <https://doi.org/10.1016/j.envsoft.2012.09.003>.
- Lefebvre W, Vercauteren J, Schrooten L, Janssen S, Degraeuwe B, Maenhaut W, et al. 2011. Validation of the MIMOSA-AURORA-IFDM model chain for policy support: modeling concentrations of elemental carbon in Flanders. *Atmos Environ* 45(37):6705–6713, <https://doi.org/10.1016/j.atmosenv.2011.08.033>.
- Brauer M, Hoek G, van Vliet P, Meliefste K, Fischer P, Gehring U, et al. 2003. Estimating long-term average particulate air pollution concentrations: application of traffic indicators and geographic information systems. *Epidemiology* 14(2):228–239, PMID: 12606891, <https://doi.org/10.1097/01.EDE.0000041910.49046.9B>.
- Cesaroni G, Porta D, Badaloni C, Stafoggia M, Eeftens M, Meliefste K, et al. 2012. Nitrogen dioxide levels estimated from land use regression models

- several years apart and association with mortality in a large cohort study. *Environ Health* 11:48, PMID: 22808928, <https://doi.org/10.1186/1476-069X-11-48>.
31. Henderson SB, Beckerman B, Jerrett M, Brauer M. 2007. Application of land use regression to estimate long-term concentrations of traffic-related nitrogen oxides and fine particulate matter. *Environ Sci Technol* 41(7):2422–2428, PMID: 17438795, <https://doi.org/10.1021/es0606780>.
 32. Luo H, Zhang Q, Yu K, Meng X, Kan H, Chen R. 2022. Long-term exposure to ambient air pollution is a risk factor for trajectory of cardiometabolic multimorbidity: a prospective study in the UK biobank. *EBioMedicine* 84:104282, PMID: 36174399, <https://doi.org/10.1016/j.ebiom.2022.104282>.
 33. Rosenlund M, Forastiere F, Stafoggia M, Porta D, Perucci M, Ranzi A, et al. 2008. Comparison of regression models with land-use and emissions data to predict the spatial distribution of traffic-related air pollution in Rome. *J Expo Sci Environ Epidemiol* 18(2):192–199, PMID: 17426734, <https://doi.org/10.1038/sj.jes.7500571>.
 34. Blom G. 1961. Statistical estimates and transformed beta-variables. *Biom J* 3:285.
 35. Whitfield JB. 2001. Gamma glutamyl transferase. *Crit Rev Clin Lab Sci* 38(4):263–355, PMID: 11563810, <https://doi.org/10.1080/20014091084227>.
 36. Yang W-Y, Zhang Z-Y, Thijs L, Bijens EM, Janssen BG, Vanpoucke C, et al. 2017. Left ventricular function in relation to chronic residential air pollution in a general population. *Eur J Prev Cardiol* 24(13):1416–1428, PMID: 28617090, <https://doi.org/10.1177/2047487317715109>.
 37. Valeri L, VanderWeele TJ. 2015. SAS macro for causal mediation analysis with survival data. *Epidemiology* 26(2):e23–e24, PMID: 25643116, <https://doi.org/10.1097/EDE.0000000000000253>.
 38. Horvath S. 2013. DNA methylation age of human tissues and cell types. *Genome Biol* 14(10):R115, PMID: 24138928, <https://doi.org/10.1186/gb-2013-14-10-r115>.
 39. Nwanaji-Enwerem JC, Dai L, Colicino E, Oulhote Y, Di Q, Kloog I, et al. 2017. Associations between long-term exposure to PM2.5 component species and blood DNA methylation age in the elderly: the VA normative aging study. *Environ Int* 102:57–65, PMID: 28284819, <https://doi.org/10.1016/j.envint.2016.12.024>.
 40. Rutledge J, Oh H, Wyss-Coray T. 2022. Measuring biological age using omics data. *Nat Rev Genet* 23(12):715–727, PMID: 35715611, <https://doi.org/10.1038/s41576-022-00511-7>.
 41. Wang C, Koutrakis P, Gao X, Baccarelli A, Schwartz J. 2020. Associations of annual ambient PM2.5 components with DNAm PhenoAge acceleration in elderly men: The Normative Aging Study. *Environ Pollut* 258:113690, PMID: 31818625, <https://doi.org/10.1016/j.envpol.2019.113690>.
 42. Baranyi G, Deary IJ, McCartney DL, Harris SE, Shortt N, Reis S, et al. 2022. Life-course exposure to air pollution and biological ageing in the Lothian Birth Cohort 1936. *Environ Int* 169:107501, PMID: 36126422, <https://doi.org/10.1016/j.envint.2022.107501>.
 43. Pope CA 3rd, Bhatnagar A, McCracken JP, Abplanalp W, Conklin DJ, O'Toole T. 2016. Exposure to fine particulate air pollution is associated with endothelial injury and systemic inflammation. *Circ Res* 119(11):1204–1214, PMID: 27780829, <https://doi.org/10.1161/CIRCRESAHA.116.309279>.
 44. Risom L, Møller P, Loft S. 2005. Oxidative stress-induced DNA damage by particulate air pollution. *Mutat Res* 592(1–2):119–137, PMID: 16085126, <https://doi.org/10.1016/j.mrfmmm.2005.06.012>.
 45. van Eeden SF, Tan WC, Suwa T, Mukae H, Terashima T, Fujii T, et al. 2001. Cytokines involved in the systemic inflammatory response induced by exposure to particulate matter air pollutants (PM(10)). *Am J Respir Crit Care Med* 164(5):826–830, PMID: 11549540, <https://doi.org/10.1164/ajrccm.164.5.2010160>.
 46. Liu T, Zhang L, Joo D, Sun SC. 2017. NF-κB signaling in inflammation. *Signal Transduct Target Ther* 2:17023–17023, PMID: 29158945, <https://doi.org/10.1038/sigtrans.2017.23>.
 47. Niranjani R, Thakur AK. 2017. The toxicological mechanisms of environmental soot (black carbon) and carbon black: focus on oxidative stress and inflammatory pathways. *Front Immunol* 8:763, PMID: 28713383, <https://doi.org/10.3389/fimmu.2017.00763>.
 48. Franceschi C, Bonafè M, Valensin S, Olivieri F, De Luca M, Ottaviani E, et al. 2000. Inflamm-aging. An evolutionary perspective on immunosenescence. *Ann NY Acad Sci* 908:244–254, PMID: 10911963, <https://doi.org/10.1111/j.1749-6632.2000.tb06651.x>.
 49. Ferrucci L, Fabbri E. 2018. Inflammageing: chronic inflammation in ageing, cardiovascular disease, and frailty. *Nat Rev Cardiol* 15(9):505–522, PMID: 30065258, <https://doi.org/10.1038/s41569-018-0064-2>.
 50. Calvo MS, Eyre DR, Gundberg CM. 1996. Molecular basis and clinical application of biological markers of bone turnover. *Endocr Rev* 17(4):333–368, PMID: 8854049, <https://doi.org/10.1210/edrv-17-4-333>.
 51. Schurgers LJ, Cranenburg EC, Vermeer C. 2008. Matrix gla-protein: the calcification inhibitor in need of vitamin K. *Thromb Haemost* 100(4):593–603, PMID: 18841280.
 52. Weber P. 2001. Vitamin K and bone health. *Nutrition* 17(10):880–887, PMID: 11684396, [https://doi.org/10.1016/s0899-9007\(01\)00709-2](https://doi.org/10.1016/s0899-9007(01)00709-2).
 53. LeBlanc JG, Milani C, de Giori GS, Sesma F, van Sinderen D, Ventura M. 2013. Bacteria as vitamin suppliers to their host: a gut microbiota perspective. *Curr Opin Biotechnol* 24(2):160–168, PMID: 22940212, <https://doi.org/10.1016/j.copbio.2012.08.005>.
 54. Ichihashi T, Takagishi Y, Uchida K, Yamada H. 1992. Colonic absorption of menaquinone-4 and menaquinone-9 in rats. *J Nutr* 122(3):506–512, PMID: 1542008, <https://doi.org/10.1093/jn/122.3.506>.
 55. Shea MK, Booth SL, Massaro JM, Jacques PF, D'Agostino RB, Dawson-Hughes B, et al. 2008. Vitamin K and vitamin D status: associations with inflammatory markers in the Framingham Offspring Study. *Am J Epidemiol* 167(3):313–320, PMID: 18006902, <https://doi.org/10.1093/aje/kwm306>.
 56. Dihingia A, Ozah D, Baruah PK, Kalita J, Manna P. 2018. Prophylactic role of vitamin K supplementation on vascular inflammation in type 2 diabetes by regulating the NF-κB/Nrf2 pathway via activating Gla proteins. *Food Funct* 9(1):450–462, PMID: 29227493, <https://doi.org/10.1039/c7fo01491k>.
 57. Vervoort LM, Ronden JE, Thijssen HH. 1997. The potent antioxidant activity of the vitamin K cycle in microsomal lipid peroxidation. *Biochem Pharmacol* 54(8):871–876, PMID: 9354587, [https://doi.org/10.1016/s0006-2952\(97\)00254-2](https://doi.org/10.1016/s0006-2952(97)00254-2).
 58. Li J, Wang H, Rosenberg PA. 2009. Vitamin K prevents oxidative cell death by inhibiting activation of 12-lipoxygenase in developing oligodendrocytes. *J Neurosci Res* 87(9):1997–2005, PMID: 19235890, <https://doi.org/10.1002/jnr.22029>.
 59. Mishima E, Ito J, Wu Z, Nakamura T, Wahida A, Doll S, et al. 2022. A non-canonical vitamin K cycle is a potent ferroptosis suppressor. *Nature* 608(7924):778–783, PMID: 35922516, <https://doi.org/10.1038/s41586-022-05022-3>.
 60. Wei F-F, Drummen NEA, Schutte AE, Thijs L, Jacobs L, Petit T, et al. 2016. Vitamin K dependent protection of renal function in multi-ethnic population studies. *EBioMedicine* 4:162–169, PMID: 26981580, <https://doi.org/10.1016/j.ebiom.2016.01.011>.